

OBJECTIVE ANALYSIS OF ENVIRONMENTAL CONDITIONS ASSOCIATED WITH SEVERE THUNDERSTORMS AND TORNADOES¹

R. M. ENDLICH and R. L. MANCUSO

Stanford Research Institute, Menlo Park, Calif.

ABSTRACT

This study describes objective analysis of the atmospheric conditions that precede or accompany severe thunderstorms and tornadoes. The data used are standard rawinsonde observations and hourly surface reports as they are transmitted over teletypewriter. In analyzing upper air data, spherical coordinates are used with grid points $2\frac{1}{2}^\circ$ of lat. and long. apart. Hourly observations are analyzed on a $1\frac{1}{4}^\circ$ grid. The vertical structure of the atmosphere is represented by seven layers between the surface and 100 mb. Observational data are averaged for these layers using all points in the soundings. By use of a nondimensional pressure term as the vertical coordinate, the three layers below 500 mb. slope with the terrain, and the lowest layer contains most boundary processes.

The objective analysis procedure fits a first degree polynomial to at least five observations that are nearest to a grid point. A distance weighting factor and upstream-downstream enhancement are used. The analysis method smooths the observations lightly, but has a resolution and accuracy that appear approximately equivalent to those of hand methods. Analyzed quantities include wind components, height, temperature, and moisture. From these a number of kinematic quantities not normally available to forecasters are computed and compared with storm developments. In general, certain quantities that depend on the field of motion appear to be more directly related to storm formation than do synoptic or thermodynamic factors. Objective severe storm indicators that combine different synoptic or kinematic factors are formulated at grid points, and their patterns match areas of storm development reasonably well. The results support the belief that the forecaster's accuracy and efficiency can be increased through greater reliance on computer methods of data processing and analysis.

SYMBOLS

| | |
|--------------------|---|
| z | Height of a constant pressure surface (m.) |
| p | Pressure (mb.) |
| P | Nondimensional pressure in Sangster's system, $P = 5[(p - 500)/(p_{sf} - 500) + 1]$ |
| T, M | Temperature and dew point, °C. (°F. in hourly data) |
| u, v | Eastward and northward wind components (m. sec. ⁻¹) |
| w | Vertical motion (cm. sec. ⁻¹) |
| \mathbf{V} | Horizontal wind vector (m. sec. ⁻¹) |
| x, y, z | Coordinate axes eastward, northward, and upward |
| Δy | Distance increment taken as 2.5° lat. or 277.8 km. for the upper air grid, and half this distance for the surface grid |
| Δx | Distance increment taken as $\Delta y \cos \phi$ |
| Δz | Layer thickness (m.) |
| ζ | Relative vorticity, $\Delta v/\Delta x - \Delta u/\Delta y$, 10^{-5} sec. ⁻¹ |
| D | Divergence $\Delta u/\Delta x + \Delta v/\Delta y$, 10^{-5} sec. ⁻¹ |
| Def | Resultant deformation $[(\Delta u/\Delta x - \Delta v/\Delta y)^2 + (\Delta v/\Delta x + \Delta u/\Delta y)^2]^{1/2}$, 10^{-5} sec. ⁻¹ |
| ∇, ∇^2 | Horizontal gradient operator and Laplacian operator |
| ξ | Frontogenesis (accumulation) of temperature (and dew point) $-\mathbf{n} \cdot [(\partial T/\partial x)\nabla u + (\partial T/\partial y)\nabla v]$ where \mathbf{n} is a unit vector perpendicular to isotherms, $10^{-12}^\circ\text{C. m.}^{-1} \text{ sec.}^{-1}$ |

| | |
|-----------------|---|
| S_1, S_2, S_3 | Three indicators of severe storm activity based on the sums of different factors |
| W | Weighting factor, inversely proportional to distance between observation and grid point, used in objective analysis |
| \mathbf{R} | Position vector from a grid point to an observing station |

1. INTRODUCTION

Among research meteorologists concerned with severe thunderstorms and tornadoes, there appears to be substantial agreement concerning the need for objective techniques of analysis and forecasting, insofar as these can be applied (e.g., House [7], Newton [11], Foster [4]). In this study, an attempt is made to formulate appropriate methods of objective analysis, to apply the methods to standard (i.e., teletypewritten) hourly and upper air data, to determine environmental conditions that precede and accompany severe storms, and to estimate the potential value of objective methods in operational use.

At the beginning of the study, conversations were held with forecasters of the National Severe Storms Forecast Center at Kansas City, Mo., concerning recent operational practices, and with research personnel of the National Severe Storms Laboratory at Norman, Okla., concerning basic studies in progress there [8]. The research program described below is based on these contacts, on recent literature, and on discussions with personnel of the Techniques Development Laboratory at Silver Spring, Md.

¹ This work was carried out under Contract Cwb-11293 with the Environmental Science Services Administration.

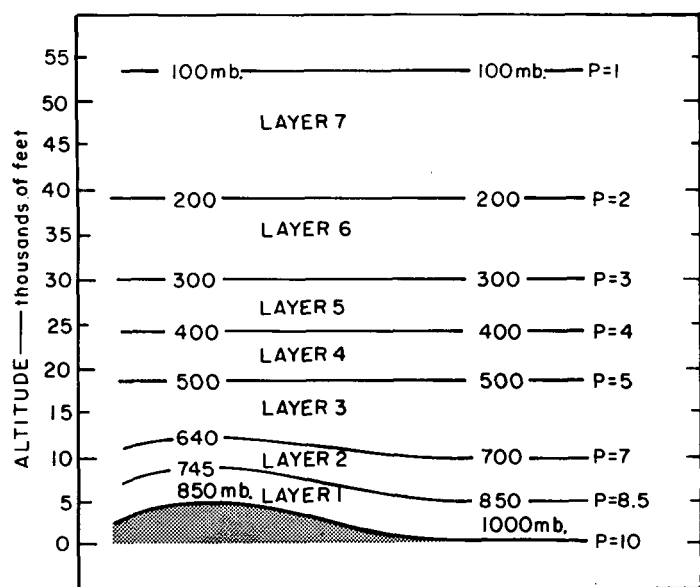


FIGURE 1.—Layers used in objective analysis based on Sangster's [13] vertical coordinate system.

2. OBJECTIVE ANALYSIS METHODS

Analysis methods for severe storms should portray detailed flow features and retain spatial gradients as indicated by observations with only a slight smoothing. Also, it seemed desirable to us to avoid assumptions of quasi-geostrophic balance and adiabatic motion that are commonly made in hemispheric analyses, but do not apply to squall lines and thunderstorms. In accord with this approach, the analysis of winds, temperature, and moisture was of greater concern than pressure-height analysis, and will be emphasized in the subsequent discussion.

VERTICAL LAYERS AND HORIZONTAL GRIDS

For upper air analysis, the vertical structure of the atmosphere is represented by seven layers between the surface and 100 mb. In each layer, a meteorological quantity (temperature, humidity, or wind component) used in the subsequent analysis is taken as an average of all mandatory and significant sounding points that lie within the layer. The trapezoidal rule is used for the integration with pressure as the vertical coordinate. In this way all points of the sounding are used, and at the same time the number of bits of information is considerably reduced. Calculations of divergence, vorticity, vertical motion, frontogenesis, etc. in the free atmosphere are made using the layer-averaged quantities which are believed to be more representative than observations at isolated standard levels (such as 850 or 700 mb.).

The selection of the number of layers and of layer boundaries is arbitrary. The first layer was chosen to encompass the earth's boundary layer, which is usually considered to lie within the first 1.5 km., approximately, above the earth's surface. Since the terrain slope in the United States is appreciable, a constant pressure surface (such as the 800-mb. level) is a poor approximation to the

top of the boundary layer. However, layers defined in Sangster's [13] coordinate system conform to the terrain in the layers below 500 mb.; this system has been employed in this study. Figure 1 shows the layers used, along with typical pressures at layer boundaries. Over high terrain, the layers below 500 mb. are thinner than elsewhere. This system is convenient for kinematic computations based on winds, but has the minor drawback that representation of the quasi-horizontal pressure force in the lowest three layers is rather complex, as discussed by Sangster.

The main limitation that exists on the horizontal resolution of upper air analyses arises from the distribution of observations in space and time. There are approximately 70 upper air stations in the conterminous United States, and our experience indicates that the grid should contain at least twice as many points as stations in order to represent the fields adequately. A grid spacing of about 125 mi. contains approximately this number of points. Since a spherical grid is simple and convenient, we chose this system with grid points at $2\frac{1}{2}^\circ$ lat. and long. intersections. For analysis of the more numerous surface hourly observations, a grid with a $1\frac{1}{4}^\circ$ spacing was used. Unfortunately, the smaller portion of the mesoscale spectrum is not adequately represented by the data spacing or by these grids, but this is unavoidable.

USE OF OPERATIONAL DATA

Difficult problems were encountered in using operational teletypewriter data. Our first approach was to obtain standard data recorded on magnetic tapes. Then programmers were assigned to decode the information and place it in a convenient format. After considerable effort, it became clear that within available time we would not be successful in this attempt. Most of the difficulties involved are inherent in teletypewriter data—namely complicated formats, noncomputer symbols, different message lengths from station to station, variable order, etc. Also, present codes conceal errors made in computation and in transmission, and these are troublesome in objective analysis. Another fault of present codes is that wind directions are given only in 10° increments even though the basic accuracy of the measurements is better than this. In short, there is a serious gap between computer usage and archaic weather codes. The action taken was to keypunch hourly and upper air data from printed teletypewriter sheets onto IBM cards in a format that preserved the structure of the information. Three different cases of severe storms were studied in detail. The first case is that of Apr. 27 and 28, 1966, when a family of tornadoes occurred in eastern Oklahoma. The second case is for June 8 and 9, 1966, and culminated in the destructive Topeka, Kans., tornado that has been discussed by Galway [5]. This case is described later. The third case is for Oct. 14 and 15, 1966, when numerous tornadoes occurred in Iowa and Missouri. Since these cases span different seasons and different areas, we believe that they permit one to make fairly reliable judgments of the objective analyses.

OBJECTIVE ANALYSIS TECHNIQUE

The analysis method (formulated by Mancuso) incorporates features similar to those used by Panofsky [12], Gilchrest and Cressman [6], and McDonell [9], including the following:

1) The basic procedure fits a first degree polynomial by least squares to observations of a scalar quantity (such as z , T , u , v) at the five stations nearest to a grid point. The value at the grid point is determined from the polynomial. This method gives some smoothing since it cannot fit the observations exactly. It has the feature of fitting an isolated observation closely, but gives an average value of clustered observations. Such clustering occurs in surface observations around certain cities, and also where one analyzes between an isolated ocean station and the mainland. A first guess based on a forecast or a previous analysis is not used, although this feature might be desirable over sparse data areas, or if observations closely spaced in time were used.

2) To avoid oversmoothing and to make the analyzed grid point values agree most closely with the nearest stations, a distance weighting factor W for each observation is included in the least squares fitting process. For example in the temperature analysis, the quantity $\Sigma W(T_0 - T_p)^2$ is minimized (where T_0 is the observed temperature and T_p is the polynomial estimate). The weighting factor is made inversely proportional to distance by using

$$W = C^2 / [(R + R^*)^2 + C^2]$$

where C^2 is a constant, and R is the distance (measured in units of degrees of latitude) from the grid point to the observation. R^* is a distance factor that measures whether the observation is in an upwind-downwind direction or in a crosswind direction from the grid point. It is computed as the magnitude of $\mathbf{k} \cdot \mathbf{R} \times \mathbf{V} / V$ where \mathbf{R} is the position vector from the grid point to the observation and \mathbf{V} is the observed wind. R^* has a magnitude between zero and R . Use of this factor gives upwind-downwind observations greater weight than crosswind observations. This feature tends to align isolines of the analyzed scalar with the flow direction. It is in general accord with hand analysis procedures and with space correlation functions that fall off more rapidly crosswind than along the wind [1]. The C^2 values presently used (6 for upper air analysis and 3 for surface analysis) were chosen to provide smoothing comparable to hand analyses of the same data.

3) To account for the effect of uneven surface data distributions, a test is made of distances between the five selected stations. If any two of the stations are closer than 30 mi., an additional station (the next nearest) is selected and included in the analysis.

4) Although this technique performed well in areas of good data coverage, it sometimes gave erratic results around the edges of the area—i.e., the adjacent oceans. This problem was partially resolved by averaging the five

weighted observations and assigning this averaged value to the grid point. This is treated as an additional observation and is included in the fitting process with a low weight. In areas of sparse data it is relatively important in establishing the grid point value, whereas in other areas it has little influence.

For the upper air analysis, a grid point value of a quantity represents a volume average since it has been determined by a process which includes both vertical and horizontal smoothing. For surface data, a grid point value is an areal average.

The analyzed fields compare well with carefully prepared hand analyses except around the edges of the grid where data are sparse and the human applies pattern recognition concepts not duplicated in the objective procedure. The objective analyses can be evaluated also on the basis of the smoothness of their horizontal derivatives. For example, acceptable wind analyses should have rather regular patterns of divergence and vorticity. This matter can be judged from figures given later.

KINEMATIC COMPUTATIONS

From the grid point analyses of meteorological quantities, fields of certain basic kinematic quantities were computed so that their patterns and changes with time could be compared with the development of severe storms, with the purpose of isolating factors useful in analysis and forecasting. The quantities divergence, vorticity, deformation, and frontogenetical effects were computed in each layer using centered space differences of the pertinent variables. In these calculations, terms like $(v/r) \tan \phi$ (which arise due to the use of spherical coordinates) were neglected due to their negligible magnitude in comparison to errors in the observations and analyses. Similarly, the horizontal divergence of the two quantities MV and TV were computed. The significance of the first of these can be understood by using the vector identity $\nabla \cdot (MV) = \mathbf{V} \cdot \nabla M + M(\nabla \cdot \mathbf{V})$. This expression tends to have largest negative values under conditions of advection of moist air (first term on the right negative) and horizontal convergence (second term negative). Thus it is a measure of an inflow of moist air, and of upward motion in the lower layers which can release the latent energy. Similarly, negative values of $\nabla \cdot (TV)$ favor release of conditional instability. Also, vertical vector wind shear, lapse rate, and destabilizing temperature advection were computed between the low and middle troposphere (Layer 1 to Layer 4), and the temperature gradient at the tropopause level (Layers 6 and 7) was found. Vertical motion was calculated at layer boundaries from the continuity equation in the form

$$\rho_t w_t - \rho_b w_b = [(\rho u \Delta z)_E - (\rho u \Delta z)_W] / (2\Delta x) + [(\rho v \Delta z)_N - (\rho v \Delta z)_S] / (2\Delta y).$$

Here the local change of density $(\partial \rho / \partial t)$ has been neglected, as is frequently done. The subscript t refers to the top of a layer, b to the bottom, and N , S , E , W refer to adjacent

grid points to the north, south, east, and west. At the ground, w is zero. The vertical motion is perpendicular to layer boundaries, and therefore may depart by a degree or two from the direction of the local vertical; however, this deviation is trivial and is neglected.

In addition, special indicators were formulated and tested in an attempt to delineate objectively regions on the weather map that synoptic meteorologists have found to be susceptible to severe storms. One of these is the northern portion of the region that lies between the axis of the low level temperature tongue and the axis of the low level moisture tongue. This region seems to be fairly successfully represented by an indicator defined in Layer 1 as $-(\nabla^2 T + \nabla^2 M)$. Another synoptic feature of interest is the axis of the ridge in the mean temperature field between 850 and 500 mb. Since this axis is normally oriented north-south, it can be identified by large positive values of $(-\Delta^2 T / \Delta x^2)$.

OBJECTIVE SEVERE STORM INDICATORS

Because the preparation of subjective analyses and interpretations of upper air data in regard to severe storms takes an appreciable amount of time, it is interesting to see whether approximately equivalent results can be achieved objectively and rapidly through use of the analyses and kinematic quantities mentioned above. As a preliminary test, we arbitrarily defined three different severe storm indicators, and computed each indicator at each grid point. The indicators are formulated so that grid points having most favorable conditions for severe storms have the highest positive values. The procedure is essentially a computer method of using a check list of factors, as done by forecasters [10].

The first indicator (S_1) is based on synoptic factors such as strong wind speed and high moisture content in Layer 1, relatively unstable lapse rate (Layer 1 to 4), strong high level winds (Layer 6), large gradient of temperature near the tropopause, warm advection in Layer 1, cold advection in the midtroposphere (Layer 4), and proximity to temperature and moisture axes in Layer 1. These factors are considered significant by operational meteorologists.

A second indicator (S_2) is based on the particular combination of synoptic factors identified as important by Crumrine [2]. One factor is destabilizing temperature advection between the low and midtroposphere (Layers 1 and 4). Another factor identifies a location that meets three criteria, namely, it is on the 4260 m. thickness line (850–500 mb.), is about 100 mi. west of the thickness ridge line, and lies in maximum anticyclonic shear of the vertical wind shear vector between the low and middle troposphere. In the objective formulation, the advection is evaluated from winds and temperature rather than by geostrophic hodograph analysis as used by Crumrine.

The third storm indicator (S_3) is based on kinematic quantities, including positive vertical motion at the top of Layer 1, convergence of the moisture flux in Layer 1,

vorticity production (divergence times vorticity) in Layer 1, a destabilizing vertical distribution of $\nabla \cdot (TV)$, and high level divergence (Layer 6). Comparisons of the three indicators will be given later.

The indicators are formulated in the following way. Since the factors of interest have different units and magnitudes, we first made each one nondimensional by dividing its value at a grid point by its approximate standard deviation. For example if D is low level divergence, we used $D/\sigma(D)$ as the first factor. Since different factors have different signs when favorable to severe storms, we multiply each factor by m_i , which is taken appropriately as $+1$ or -1 . An individual quantity F_i thus becomes $m_i F_i / \sigma_i$. (If the relative merits of different factors were known, this effect could be introduced by varying the magnitude of m_i .) The factors used in an indicator S are summarized as

$$S = \sum_{i=1}^n m_i F_i / \sigma_i.$$

If all factors are favorable at a grid point, S will have relatively large values. If one factor is in the wrong sense (for example, divergence instead of convergence), the indicator is decreased. The three different forms of S are simply arbitrary numbers whose patterns indicate the areas of relatively high probability of severe storms. The magnitude of S may be useful also, but this can only be established after study of many cases. When an individual factor ($m_i F_i / \sigma_i$) is favorable, it will have a value on the order of 1 to 2, say $(1+\epsilon)$. Therefore, the sum in the most favorable case will have a magnitude of approximately $(1+\epsilon)n$, where n is the number of factors. To eliminate this dependence on n , the indicators could be normalized further by dividing each by n . As a final comment, we note that in all three indicators, correlations probably exist between different factors (e.g., temperature and moisture in Layer 1). Further investigation would be required to determine an S based on an optimum combination of uncorrelated factors.

COMPUTER PROGRAMS

The programs that were written are listed below.

1) The first program decodes a standard rawinsonde message, computes layer boundaries in Sangster's system, and computes layer averaged values of $z, P, T, M, \rho, u, v, \Delta z, \rho u \Delta z$, and $\rho v \Delta z$. The running time is approximately 2 sec. per station.

2) The second program is for objective analysis. This requires approximately 110 sec. to analyze nine quantities for each of seven layers—i.e., approximately 2 sec. per chart.

3) The third program computes a number of kinematic quantities. These include divergence, vorticity, deformation, frontogenesis, convergence of moisture flux, temperature advection, geostrophic winds and departures, and vertical motion. Running time is approximately 3 sec. per chart.

4) The fourth program computes the three objective storm indicators described earlier in a manner analogous to a forecaster's use of a check list.

3. TORNADO CASE OF JUNE 8-9, 1966

This section contains selected charts showing quantities that appear to be most closely related to severe storm development. The grid point computations were printed out in a rectangular array, and a base map was fitted to the printout. The printed numbers are rounded to integers, but the decimals were retained in computations. Wind analyses in vector form and isolines on various charts were drawn by hand to facilitate inspection.

The tornadoes and funnels reported for this case are shown in figure 2, as taken from *Storm Data* published by the National Weather Records Center. Positions in chronological order are given by numbers between 1 and 16. The first tornado occurred in Colorado at 0900 GMT

on June 8. Numerous tornadoes and funnels were observed in Kansas and Oklahoma between 1700 GMT on the 8th and 0300 GMT on the 9th. The number 11 indicates the highly destructive Topeka, Kans., tornado. In addition, tornadoes occurred near Miami in association with hurricane Anna, which was in the Gulf of Mexico. Large hail occurred in Illinois. Later on, tornadoes occurred near Chicago and in southern Michigan.

The boundary layer wind analysis at 1200 GMT on June 8 (fig. 3) shows the vortex center with which the tornadoes were associated located near 39°N., 102°W. (eastern Colorado). The resolution of the analysis is believed to be similar to that attainable by hand analysis methods. Of course the reliability is a function of the proximity of grid points to observing stations. The vertical motion field, shown in figure 4, has a typical degree of smoothness. Largest upward motion generally includes the area where severe storms formed. Magnitudes increased in intensity to about 10 cm. sec.⁻¹ at 500 mb. Above this level, they tend to become unreliable due to an

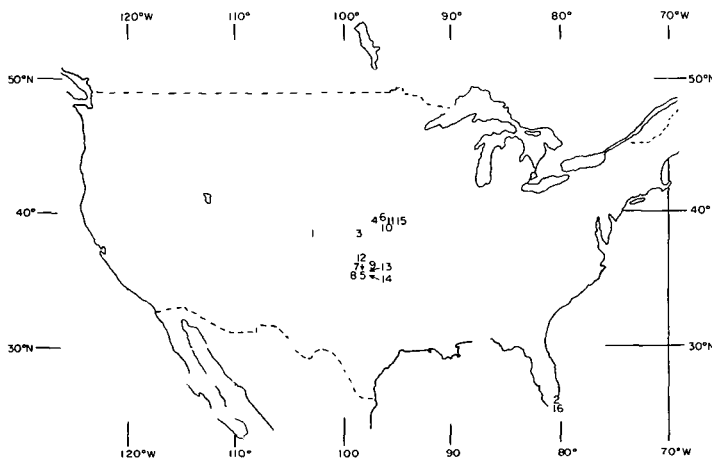


FIGURE 2.—Numbers indicate locations and chronological order of occurrence of tornadoes and funnels observed between 0900 GMT on June 8 and 0300 GMT on June 9, 1966.

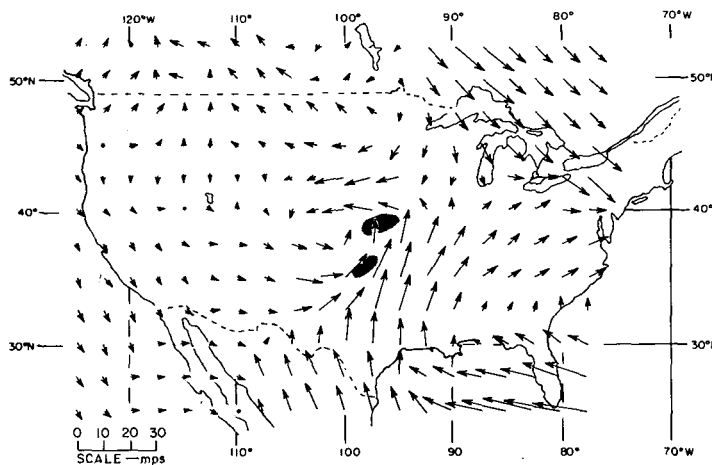


FIGURE 3.—Wind analysis in the boundary layer at 1200 GMT June 8, approximately 5 hr. before the beginning of the main tornado outbreak. Cross hatching identifies areas of multiple tornadoes.

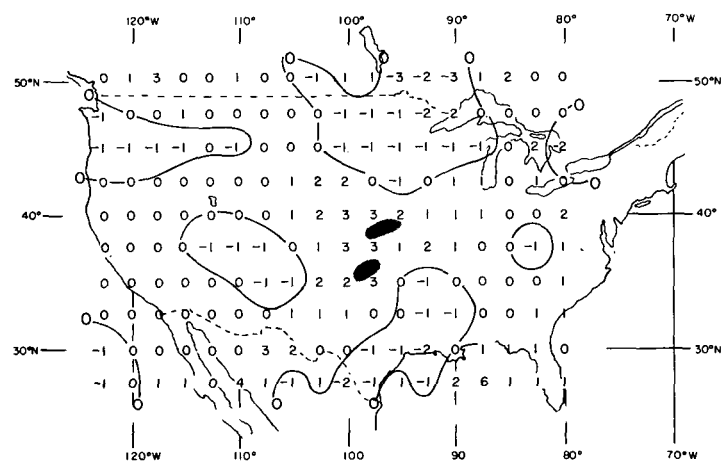


FIGURE 4.—Vertical motion (cm. sec.⁻¹) at the top of the boundary layer at 1200 GMT June 8.

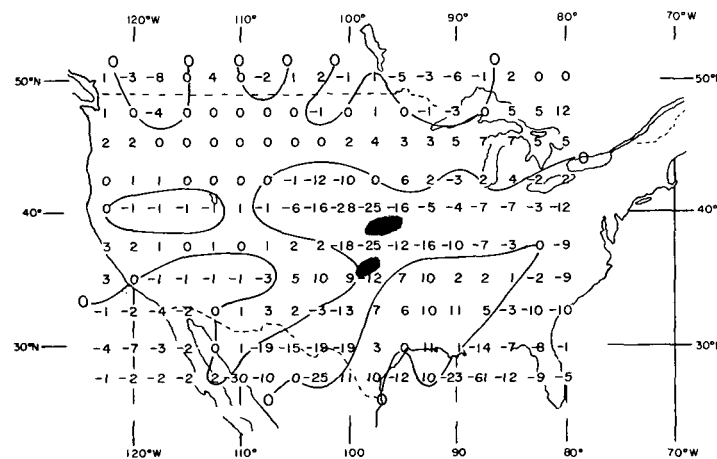


FIGURE 5.—Divergence of the moisture flux ($\nabla \cdot M V$) in the boundary layer at 1200 GMT June 8 (units $10^{-5} \text{ }^{\circ}\text{C. sec.}^{-1}$).

accumulation of errors. The value of 6 cm. sec.^{-1} in the Gulf of Mexico in figure 4 should be discounted because of the uncertainty of analysis in that region. The quantity $\nabla \cdot (MV)$ in Layer 1 (fig. 5) shows fields with large negative areas apparently favorable to severe storm development. As mentioned earlier, this term accounts for both moist air advection and convergence. Another quantity computed was $-D(f+\zeta)$, which is the term for vorticity production in the vorticity equation. Figure 6 shows that this field had maximum values in an area centered slightly west of the severe storm area. Magnitudes shown in figures 5 and 6 are similar to the other cases studied. Thus it appears that quantities of this sort that represent known physical processes can be computed objectively and relate quite well to severe storm developments. These same quantities were computed also for other layers, but in general the boundary layer quantities appear to be most directly related to severe storms.

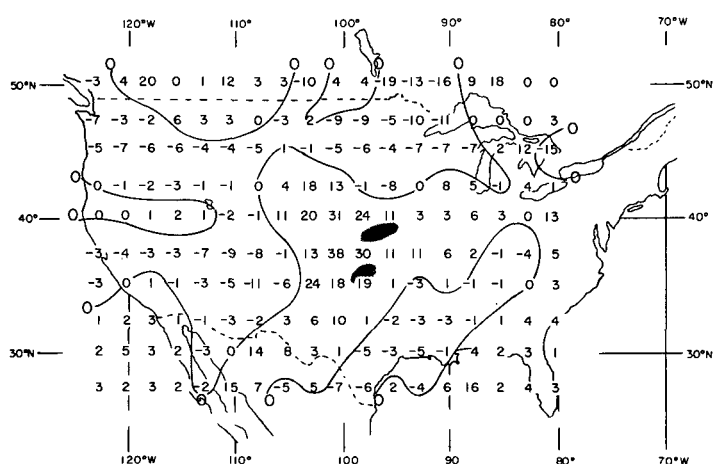


FIGURE 6.—Vorticity production term $-D(f + \zeta)$ in the boundary layer at 1200 GMT June 8 (units $10^{-10} \text{ sec.}^{-2}$).

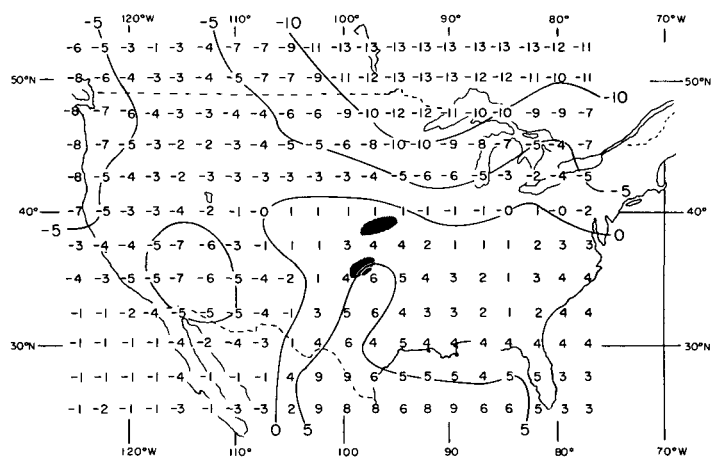


FIGURE 7.—Objective analysis of Showalter index at 1200 GMT June 8, positive values are unstable.

Other quantities of interest that involve the middle or upper troposphere will now be mentioned. One of these is the lapse rate between Layer 1 and Layer 4. This quantity is, of course, important in thermodynamic calculations related to parcel instability—i.e., warm moist air in the low levels plus a steep lapse rate is most unstable for rising parcels. An index based on these considerations is the well-known form due to Showalter [14], and the basic concept has several variations. This quantity is shown in figure 7. As in other cases examined, the patterns have smooth transitions, and values somewhat more unstable than average in the severe storm areas, but relationships between instability and storm areas are not particularly strong. At this time, and also 12 hr. later, the most unstable air lay south of the storm area. This suggests to us that the low level temperature and moisture fluxes are more directly related to severe storms than is lapse rate and parcel instability. One of the quantities found impor-

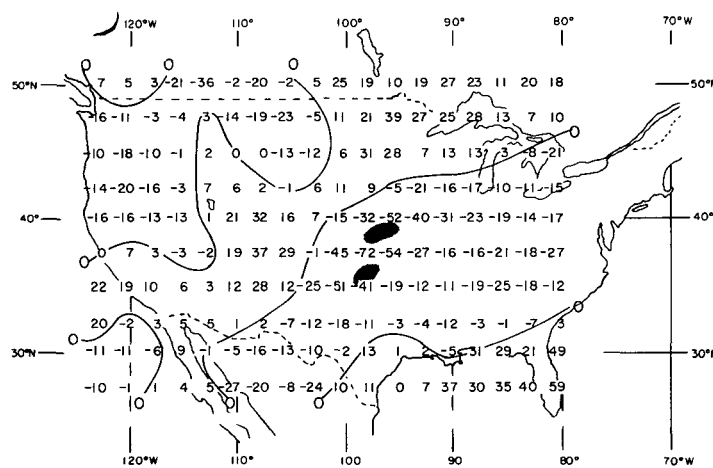


FIGURE 8.—Relative vorticity of the wind shear vector between low and midtroposphere (Layers 1 and 4), at 1200 GMT June 8 (units $10^{-6} \text{ sec.}^{-1}$).

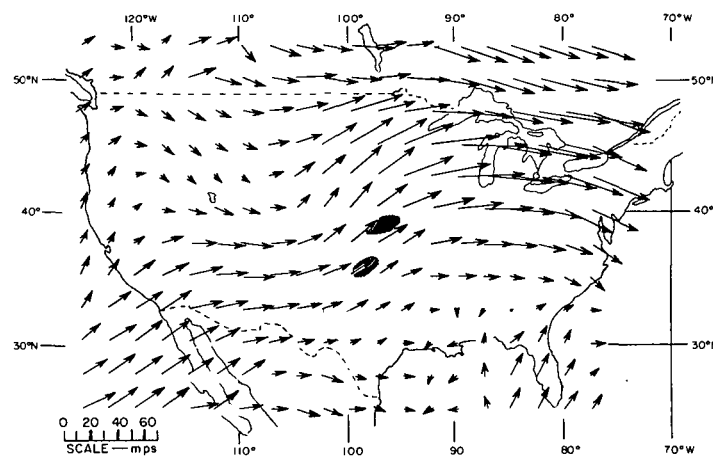
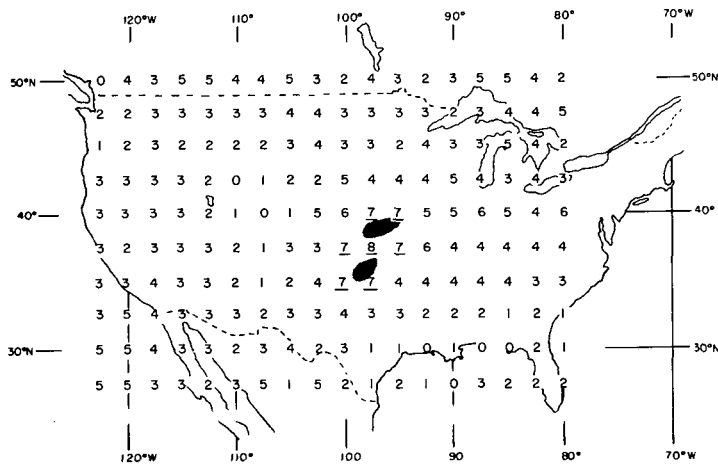
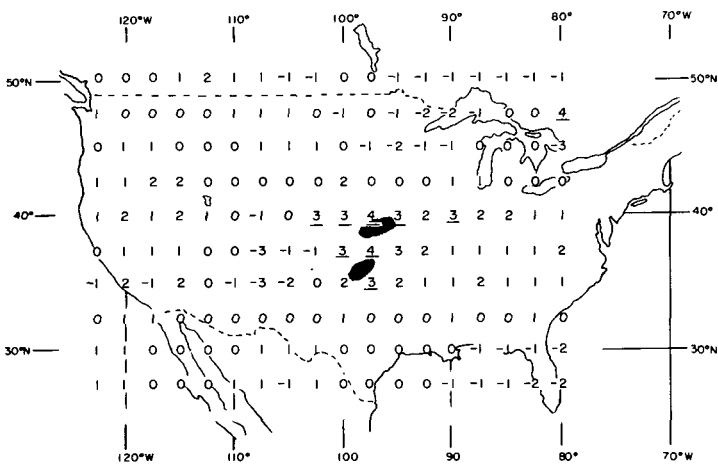
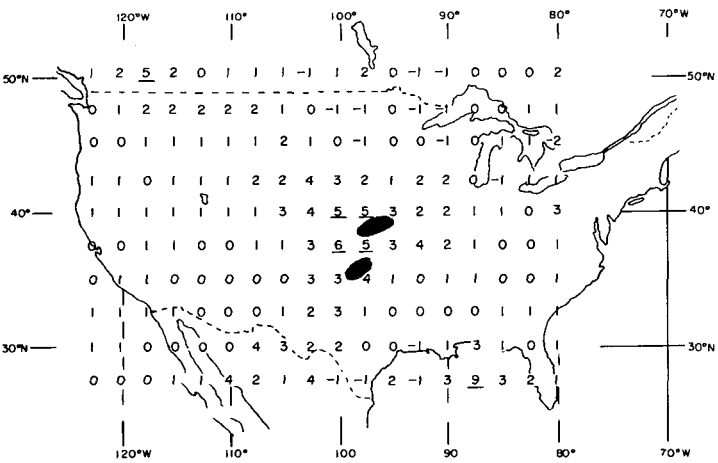


FIGURE 9.—Wind analysis in Layer 6 (300-200 mb.) at 1200 GMT June 8.

FIGURE 10.—Objective storm indicator S_1 at 1200 GMT June 8.FIGURE 11.—Objective storm indicator S_2 at 1200 GMT June 8.FIGURE 12.—Objective storm indicator S_3 at 1200 GMT June 8.

tant by Crumrine is anticyclonic horizontal shear of the wind shear vector between 850 and 500 mb. An objective criterion for this quantity is based on negative values of the relative vorticity of the shear winds between Layers 1 and 4. This quantity is shown in figure 8. Large negative values match the tornado area fairly well.

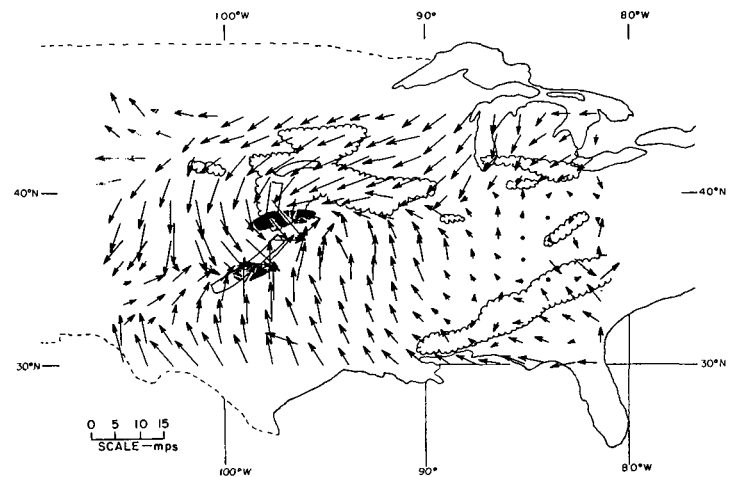
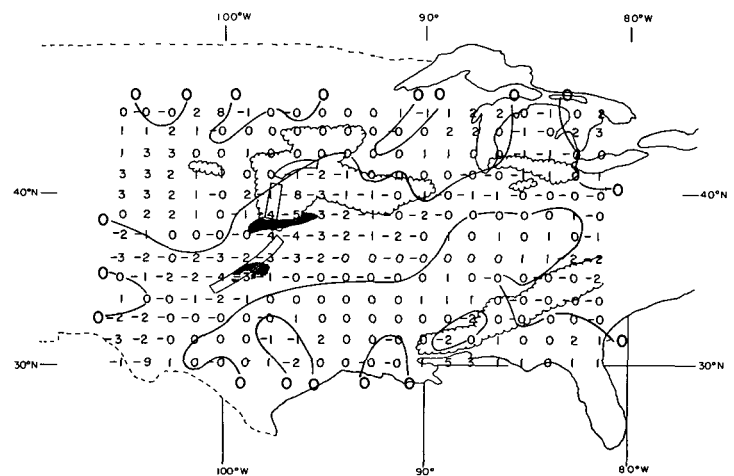


FIGURE 13.—Surface winds at 0000 GMT June 9 near the end of the tornado outbreak. Cross hatching indicates areas of multiple tornadoes. Radar echoes are shown by conventional symbols.

FIGURE 14.—Divergence of surface winds at 0000 GMT June 9 (units 10^{-5} sec^{-1}).

At this point it is pertinent to show the analyzed wind field in an upper tropospheric layer, to illustrate the relation of the jet stream to the severe storm areas (fig. 9). The strongest winds were over the Great Lakes. An upper trough and moderate jet stream (for the season) were approaching the area where severe storms occurred. Thus, this particular case conforms well to accepted patterns of upper winds.

Figures 10, 11, and 12 show the three storm indicators S_1 , S_2 , and S_3 prior to the main tornado outbreak. Their patterns match the shaded areas fairly well, indicating that use of a computerized check list is a feasible approach to providing warnings of severe storms.

Surface analyses of winds, temperature, dew points, etc. were made at 3-hr. intervals from 0000 GMT on June 8 through 1200 GMT on June 9. Only selected charts for 0000 GMT on June 9 will be shown. Figure 13 shows the wind fields. The patterns are fairly smooth except in the rough terrain of the Rockies. Considering that the basic

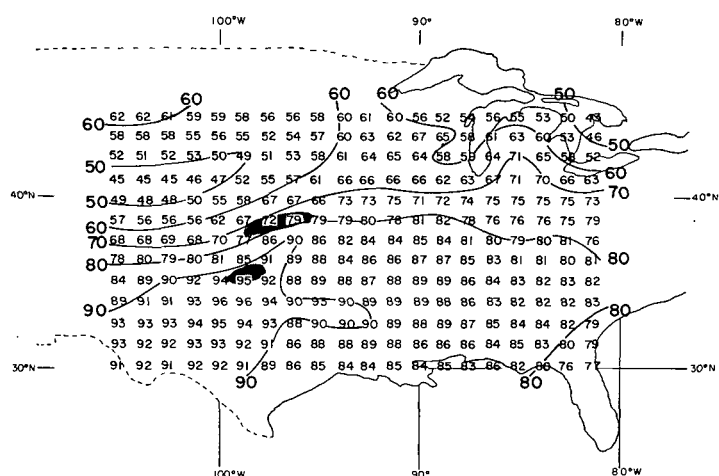


FIGURE 15.—Surface temperature (°F.) at 0000 GMT June 9.

wind data (from hourly observations) are 1-min. averages, we believe that the objective analysis is quite good. Probably more representative computations would result if the averaging period of wind observations were increased to 5 or 10 min. and greater precision were introduced in the reports of direction. Conventional radar symbols taken from radar summary maps are shown on the figures for comparison with the winds. The divergence field computed from the wind is shown in figure 14. Maximum convergence occurred in the main storm areas at the times of tornado occurrence, as expected. A grid point analysis of temperature is shown in figure 15. The packed isotherms indicate the front to which the storms are related.

Similar analyses were made of the April and October cases, and are given in [3]. In addition, for the April case an objective analysis was made of two quantities that gave quite interesting results. The first was a grid point representation of the tenths of sky covered with clouds. Patterns agree very well with concurrent satellite cloud photographs that were available. The second analysis showed the percentage of stations reporting precipitation (defined to include rain, thunderstorms, and hail) and had smooth patterns. The representation of clouds and weather in a quantitative manner of this sort appears to be advantageous for following pattern motions and for facilitating objective operations on such data.

4. DISCUSSION OF ANALYSES

Based on the June case shown above and on the two other cases that were investigated, there appeared to be considerable similarity among the types of factors that are most directly related to severe storms. In general, synoptic conditions (such as warm temperature and high dew points in low levels) cover quite large areas. The severe storms often occur in some small portion of the periphery of such areas. In our opinion patterns of parcel instability are similarly arranged. Quantities that depend on the field of motion appear to be more specific in

TABLE 1.—*Tentative rating of certain selected quantities as objective indicators of severe storm activity*

| Quantity | Rating | Remarks |
|--|----------|---|
| High wind speed in low levels..... | Poor.... | These conditions are generally present in severe storm areas, but also cover extensive regions without severe storms. Thus, they appear inferior to other quantities as indicators. |
| High temperature and humidity in low levels.. | Poor.... | |
| Large moisture gradient near 700 mb..... | Poor.... | |
| High wind speed in upper troposphere..... | Poor.... | |
| Large temperature gradient at tropopause level.. | Poor.... | |
| Unstable lapse rate between low and mid-troposphere..... | Fair.... | The most unstable lapse rate and most unstable index lie generally south of severe storm areas. |
| Unstable Showalter index..... | Fair.... | |
| Area between low level temperature and moisture axes..... | Fair.... | These axes are not always well developed. |
| Destabilizing temperature advection between low and midtroposphere..... | Good... | |
| Proximity to 4260 m.-thickness line (850-500 mb.) and to thickness ridge..... | Good... | |
| Area of negative vorticity of wind shear vector between low and midtroposphere..... | Good... | |
| Horizontal divergence in upper troposphere..... | Good... | |
| Upward vertical motion at top of boundary layer..... | Good... | |
| Negative values of $\nabla \cdot \mathbf{MV}$ and of $\nabla \cdot \mathbf{TV}$ in low levels..... | Good... | |
| Vorticity production in low levels..... | Good... | |
| Frontogenesis of temperature and of moisture in low levels..... | Good... | |
| Destabilizing distribution of $\nabla \cdot \mathbf{TV}$ between low and midtroposphere..... | Good... | |

identifying the areas of severe storm formation. Thus we have made a tentative evaluation of the association of some different quantities with severe storms (table 1). To rank these quantities more precisely and to determine an optimum combination of severe storm indicators would require examination of a larger number of cases, or a day-by-day evaluation of objective quantities by severe storm forecasters.

Of course, in addition to objective computations, there are other ways in which one might expect to improve severe storm analysis and forecasting. These include new types of measurements such as high resolution photographs from synchronous satellites, or better ground tracking equipment. Also, improvement of present weather codes and communications would probably be very beneficial. Computer processing can eliminate practically all hand plotting and analysis, and would be compatible with storing mapped output on magnetic disks or film. Such output is compatible with display on cathode-ray tubes to provide simple and rapid monitoring of severe storm developments by forecasters.

5. SUMMARY

The writers believe that the objective analysis methods are successful in depicting a variety of features of the flow with an accuracy and resolution comparable to that attainable using ordinary methods of hand analysis. There is no doubt that objective analyses can be obtained very quickly after observations are available in a suitable format for computer use. Several of the quantities computed are of basic physical importance; these include vertical motion, divergence of temperature and moisture fluxes, destabilizing advection, and frontogenetical effects. Terms of this type will probably be needed as input to

future numerical models that are applicable to severe storms. Since these quantities can only be deduced in a rough manner by pattern inspection of standard charts, it is reasonable to expect that their immediate availability to an operational meteorologist would increase his accuracy and efficiency in forecasting.

The following statements summarize specific points:

1) Objective analysis techniques for winds, temperature, moisture, and height give results that appear comparable in resolution and accuracy to those obtained by hand analysis except where data are sparse (over oceans adjacent to the United States). The objective wind analyses are believed to be particularly important in portraying the environment of severe storms. Derived kinematic quantities such as vertical motion and moisture convergence relate well to areas where severe storms develop.

2) In analyzing standard observations, a horizontal grid spacing of approximately 100 to 150 mi. is appropriate for upper air analyses, and about half this distance is suitable for surface data. Sangster's system is convenient as a vertical coordinate. Six layers between the surface and 200 mb. appear to give adequate vertical resolution.

3) Kinematic factors and synoptic rules used by forecasters may be combined into objective severe storm indicators that appear to have operational applications.

4) In our opinion, objective analyses and kinematic computations should be made available to forecasters for day-to-day use and evaluation.

ACKNOWLEDGMENTS

We are indebted to Mr. DeVer Colson of the Techniques Development Laboratory for his aid in procuring operational data for this study. The personnel of the National Severe Storms Forecast Center and the National Severe Storms Laboratory were very helpful in discussing with us problems related to severe storms. Staff officers of the U.S. Navy Fleet Numerical Weather Facility generously informed us concerning data processing techniques in use there. Colleagues of the authors in the Aerophysics Laboratory, particularly Dr. Paul A. Davis and Mr. William Viezee, gave many helpful suggestions throughout the program. Assistance in computer programming was provided by Miss Margaret Korpi. Mr. Russell Trudeau organized, edited, and supervised the key punching of teletypewriter weather reports.

REFERENCES

1. C. E. Buell, "Two-Point Variability of Wind," *Final Report*, Contract AF19(604)-7282, Kaman Nuclear, Colorado Springs July 1962, vol. 1, Ch. 1.
2. H. A. Crumrine, "The Use of the Horizontal Temperature Advection, the 850-500 Mb. Thickness and the 850-500 Mb. Shear Wind as an Aid in Severe Local Thunderstorm Forecasting," paper presented at 244th National Meeting of the American Meteorological Society, October 1965.
3. R. M. Endlich and R. L. Mancuso, "Environmental Conditions Associated with Severe Thunderstorms and Tornadoes," *Final Report*, Contract Cwb-11293, Stanford Research Institute, Menlo Park, Calif., May 1967, 106 pp.
4. D. S. Foster, "Relationship Among Tornadoes, Vorticity Acceleration and Air Mass Stability," *Monthly Weather Review*, vol. 92, No. 7, July 1964, pp. 339-343.
5. J. G. Galway, "The Topeka Tornado of 8 July 1966," *Weatherwise*, vol. 19, No. 4, Aug. 1966, pp. 144-150.
6. B. Gilchrest and G. P. Cressman, "An Experiment in Objective Analysis," *Tellus*, vol. 6, No. 6, Nov. 1954, pp. 309-318.
7. D. C. House, "Forecasting Tornadoes and Severe Thunderstorms," *Meteorological Monographs*, vol. 5, No. 27, Sept. 1963, pp. 141-156.
8. E. Kessler, "Purposes and Programs of the National Severe Storms Laboratory, Norman, Oklahoma," *Report No. 23*, National Severe Storms Laboratory, U.S. Weather Bureau, Dec. 1964, 17 pp.
9. J. E. McDonnell, "On the Objective Analysis System Used at the National Meteorological Center," *Technical Memorandum 23*, National Meteorological Center, U.S. Weather Bureau, 1962, 31 pp.
10. R. C. Miller, "Notes on Analysis and Severe-Storm Forecasting Procedures of the Military Weather Warning Center," *Technical Report 200*, Air Weather Service, U.S. Air Force, July 1967, 170 pp.
11. C. W. Newton, "Dynamics of Severe Convective Storms," *Meteorological Monographs*, vol. 5, No. 27, Sept. 1963, pp. 33-58.
12. H. A. Panofsky, "Objective Weather Map Analysis," *Journal of Meteorology*, vol. 6, No. 6, Dec. 1949, pp. 386-392.
13. W. E. Sangster, "A Method of Representing the Horizontal Pressure Force Without Reduction of Station Pressures to Sea Level," *Journal of Meteorology*, vol. 17, No. 2, Apr. 1960, pp. 166-176.
14. A. K. Showalter, "A Stability Index for Thunderstorm Forecasting," *Bulletin of the American Meteorological Society*, vol. 34, No. 6, June 1953, pp. 250-252.

[Received September 29, 1967; revised January 8, 1968]